Supporting Information for
Benchmarking non-adiabatic quantum dynamics using the molecular Tully models

Sandra Gómez,[a] Eryn Spinlove,[b] and Graham Worth[a*]

December 14, 2023

[a] Departamento de química Física, Universidad de Salamanca https://ror.org/02f40zc51, 37008, Spain
[b] Faculty of Science and Engineering, Theoretical Chemistry — Zernike Institute for Advanced Materials, Nijenborgh 4, 9747 AG, Groningen, The Netherlands
[a] Dept. of Chemistry, University College London, 20, Gordon St., London, WC1H 0AJ, g.a.worth@ucl.ac.uk.

Contents

S1 Quantum Chemistry Data Defining Ibele-Curchod Model 1

Table S1 Vibrational modes and frequencies of ethene calculated at the D_{2h} minimum energy geometry

Mode	Symmetry	ω (cm^{-1})	ω (eV)	Description
ν_1	$1b_{2u}$	887.01	0.1100	CH rock (anti)
ν_2	$1b_{2g}$	1053.72	0.1306	pyramidalisation (anti)
ν_3	$1b_{3u}$	1142.38	0.1416	pyramidalisation (sym)
ν_4	$1b_{3g}$	1342.93	0.1665	CH rock (sym)
ν_5	$1a_g$	1446.52	0.1793	CC stretch
ν_6	$1b_{1u}$	1604.80	0.1990	CH_2 bend (anti)
ν_7	$2a_g$	1782.92	0.2211	CH_2 bend (sym)
ν_8	$1a_u$	2104.59	0.2609	torsion
ν_9	$1b_{1u}$	3323.42	0.4121	CH_2 stretch (anti)
ν_{10}	$3a_g$	3343.61	0.4146	CH_2 stretch (sym)
ν_{11}	$2b_{3g}$	3400.79	0.4216	CH stretch (anti-anti)
ν_{12}	$2b_{2u}$	3426.53	0.4248	CH stretch (sym-anti)

Table S2 Optimized Cartesian coordinates (in Å) of ethene with D_{2h} symmetry calculated using SA(3)-CASSCF(2/2)/6-31G*.

C	-0.0000000011	-0.6704906441	0.0000000000
C	0.0000000011	0.6704906441	0.0000000000
H	0.9156718485	-1.2339527181	0.0000000000
H	-0.9156718493	-1.2339527198	0.0000000000
H	0.9156718493	1.2339527198	0.0000000000
H	-0.9156718485	1.2339527181	0.0000000000

Table S3 Energies of the three lowest states of ethene calculated at the D_{2h} optimised structure with SA(3)-CASSCF(2/2)/6-31G*.

	Symmetry	E (Hartree)	ΔE (eV)
S_0 (N)	A_{1g}	-78.04883756	0.0
S_1 (V)	B_{1u}	-77.67351801	10.213
S_2 (Z)	A_{1g}	-77.48851606	15.247

S2 Quantum Chemistry Data Defining Ibele-Curchod Model 2

Table S4 Vibrational modes and frequencies of DMABN calculated at the ωB97X-D3/cc-pVDZ minimum energy geometry. ip / oop: in-plnae / out-of-plane. IPh/ OOPh: in-phase / out-of-phase. r/m/am/nit: ring / methyl / amino / nitrile

.

Mode	ω (cm^{-1})	ω (eV)	Description	Mode	ω (cm^{-1})	ω (eV)	Description
v_1	50.17	0.00622	N pyramidalisation (sym)	v_{30}	192.57	0.14786	NCH ip OOPh wag
v_2	73.31	0.00909	N pyramidalisation (anti)	v_{31}	1204.61	0.14935	CH(r) ip OOPh bend
v_3	83.28	0.01033	N oop IPh wag	v_{32}	1252.97	0.15535	CC(nit) stretch
v_4	134.95	0.01673	CN ip wag	v_{33}	1296.15	0.16070	ip ring distortion
v_5	176.51	0.02188	CH_3 IPh rotation	v_{34}	1333.18	0.16529	ip ring distortion
v_6	186.87	0.02317	CH_3 OOPh rotation	v_{35}	1391.91	0.17258	CN(am) ip wag
v_7	257.00	0.03186	ip rock (CN OOPh)	v_{36}	1416.98	0.17568	CN(am) stretch
v_8	288.35	0.03575	oop rock (CN OOPh)	v_{37}	1434.17	0.17782	CH_3 OOPh umbrella
v_9	339.78	0.04213	quinoid	v_{38}	1460.61	0.18109	CH(m) oop OOPh wag
v_{10}	429.37	0.05324	ring puckering	v_{39}	1469.44	0.18219	CH(m) oop IPh wag
v_{11}	477.36	0.05919	ip rock (CN OOPh)	v_{40}	1477.95	0.18324	CH_2 OOPh scissor
v_{12}	492.69	0.06109	CH(r) CH(m) wag IPh	v_{41}	1480.33	0.18354	CH_2 IPh scissor
v_{13}	502.80	0.06234	CC(N) oop rock	v_{42}	1505.07	0.18661	CH_3 IPh wag
v_{14}	571.15	0.07081	CH(r) oop IPh wag	v_{43}	1512.19	0.18749	CH_3 OOPh wag
v_{15}	572.87	0.07103	ip ring distortion	v_{44}	1589.53	0.19708	CN(am) CC(nit) assym
v_{16}	664.39	0.08237	ip ring distortion				stretch
v_{17}	676.38	0.08386	CN(CH_3)+CC(N) OOPh	v_{45}	1641.33	0.20350	ring distortion
			stretch	v_{46}	1709.11	0.21190	ring distortion
v_{18}	751.21	0.09314	CH oop OOPh	v_{47}	2389.09	0.29621	CN(nit) stretch
v_{19}	819.72	0.10163	ring breathing	v_{48}	3017.45	0.37412	CH_3 sym OOPh stretch
v_{20}	836.95	0.10377	CH oop OOPh	v_{49}	3025.27	0.37509	CH_3 sym IPh stretch
v_{21}	852.95	0.10575	CH oop IPh	v_{50}	3093.87	0.38359	CH_3 assym OOPh stretch
v_{22}	989.78	0.12272	CH oop OOPh	v_{51}	3094.99	0.38373	CH_3 assym IPh stretch
v_{23}	991.60	0.12294	CH oop OOPh	v_{52}	3169.04	0.39291	CH(m) OOPh stretch
v_{24}	000.75	0.12408	NCH_2 sym stretch	v_{53}	3178.38	0.39407	CH(m) IPh stretch
v_{25}	024.85	0.12707	ip ring distortion	v_{54}	3220.64	0.39931	CH(r) ip OOPh stretch
v_{26}	087.14	0.13479	NCH ip IPh wag	v_{55}	3221.56	0.39943	CH(r) ip OOPh stretch
v_{27}	137.37	0.14102	NCH_2 OOPh rock	v_{56}	3250.34	0.40299	CH(r) ip OOPh stretch
v_{28}	138.07	0.14110	NCH_2 IPh rock	v_{57}	3251.10	0.40309	CH(r) ip IPh stretch
v_{29}	153.21	0.14298	CH(r) ip OOPh bend				

Table S5 Optimized Cartesian coordinates (in Å) of DMABN calculated using ωB97X-D3/cc-pVDZ.

C	3.0172032156	-1.2495342820	-0.0407263572
N	2.2965346317	-0.0007382064	0.0765362179
C	0.9227684515	0.0011669690	0.0406136174
C	0.1894664254	-1.2080894970	0.0226004573
C	-1.1951519719	-1.2024086782	0.0071562861
C	-1.9092694984	0.0019924784	0.0014527143
C	-1.1945366746	1.2061423453	0.0075358752
C	0.1903606382	1.2111666789	0.0229409050
H	0.7068836956	2.1695413596	0.0222661446
H	-1.7369287128	2.1529942369	-0.0027881064
C	-3.3461238316	0.0002457163	-0.0155114324
N	-4.5069517191	-0.0036082781	-0.0289051756
H	-1.7378729649	-2.1491549771	-0.0035165236
H	0.7051821594	-2.1669359267	0.0216071329
C	3.0207837331	1.2456860006	-0.0416260401
H	2.7557928691	1.9437474024	0.7689936831
H	4.0954954704	1.0436507981	0.0366899803
H	2.8368107703	1.7537485375	-1.0061833358
H	2.7503589489	-1.9464189769	0.7703690787
H	2.8316611564	-1.7582031336	-1.0047208524
H	4.0925332948	-1.0507503157	0.0372493490

Table S6 Energies of the three lowest states of DMABN calculated at the optimised structure with TDA-ωB97X-D3/cc-pVDZ.

	E (Hartree)	ΔE (eV)
S_0	-458.22546	0.0
S_1	-458.04415	4.933
S_2	-458.03028	5.311

S3 Quantum Chemistry Data Defining Ibele-Curchod Model 3

Table S7 Vibrational modes and frequencies of fulvene calculated at the C_{2v} minimum energy geometry with the molecule in the yz-plane. ip / oop: in-plane / out-of-plane.

Mode	Symmetry	ω (cm^{-1})	ω (eV)	Description
ν_1	$1b_1$	210.54	0.0261	oop CH_2 wag
ν_2	$1b_2$	365.40	0.0453	ip CH_2 rock
ν_3	$1a_2$	497.97	0.0617	ring pucker
ν_4	$2b_1$	625.91	0.0776	oop ring C–H
ν_5	$2a_2$	690.41	0.0856	oop ring C–H
ν_6	$1a_1$	705.73	0.0875	ring elongation
ν_7	$3b_1$	765.34	0.0949	ring oop distortion
ν_8	$3a_2$	787.69	0.0977	CH_2 torsion
ν_9	$2b_2$	855.18	0.1060	ip ring distortion
ν_{10}	$4a_2$	893.17	0.1107	oop ring C–H
ν_{11}	$4b_1$	899.61	0.1115	oop ring C–H
ν_{12}	$2a_1$	906.76	0.1124	ring stretch
ν_{13}	$3b_2$	946.81	0.1174	CH_2 ip H-rock
ν_{14}	$3a_1$	1033.30	0.1281	ring stretch
ν_{15}	$5b_1$	1041.20	0.1291	CH_2 oop H-wag
ν_{16}	$4b_2$	1175.76	0.1458	ip ring H-bend
ν_{17}	$4a_1$	1179.94	0.1463	ip ring H-bend
ν_{18}	$5b_2$	1359.11	0.1685	ip H-rock
ν_{19}	$6b_2$	1452.69	0.1801	ip ring distortion
ν_{20}	$5a_1$	1474.77	0.1828	ip ring H-bend
ν_{21}	$6a_1$	1561.53	0.1936	ip CH_2 bend
ν_{22}	$7a_1$	1638.14	0.2031	ip ring distortion + CH_2 bend
ν_{23}	$7b_2$	1690.84	0.2096	ip ring distortion
ν_{24}	$8a_1$	1778.19	0.2205	ring=CH_2 stretch
ν_{25}	$9a_1$	3339.85	0.4141	CH_2 symm stretch
ν_{26}	$8b_2$	3422.76	0.4244	CH_2 anti-symm stretch
ν_{27}	$9b_2$	3448.75	0.4276	ring-H anti-symm stretch
ν_{28}	$10a_1$	3451.28	0.4279	ring-H symm stretch
ν_{29}	$10b_2$	3474.72	0.4308	ring-H anti-symm stretch
ν_{30}	$11a_1$	3488.21	0.4325	ring-H symm stretch

Table S8 Optimized Cartesian coordinates (in Å) of fulvene calculated using SA(2)-CASSCF(6,6)/6-31G*.

C	0.0000000000	1.1795473000	-0.1211794000
C	0.0000000000	0.7405988000	-1.4006101000
C	0.0000000000	-0.7405989000	-1.4006101000
C	0.0000000000	-1.1795473000	-0.1211794000
C	0.0000000000	0.0000000000	0.7666464000
C	0.0000000000	0.0000000000	2.1154199000
H	0.0000000000	-0.9153375000	2.6777939000
H	0.0000000000	0.9153375000	2.6777939000
H	0.0000000000	-2.1928593000	0.2152754000
H	0.0000000000	-1.3524621000	-2.2726760000
H	0.0000000000	1.3524621000	-2.2726760000
H	0.0000000000	2.1928593000	0.2152754000

Table S9 Energies of the two lowest states of fulvene calculated at the C_{2v} optimised structure with SA(2)-CASSCF(6,6)/6-31G*.

	Symmetry	E (Hartree)	ΔE (eV)
S_0	A_1	-230.72231135	0.0
S_1	B_2	-230.56998243	4.161

S4 ML-MCTDH trees for LVC calculations on the IC Models

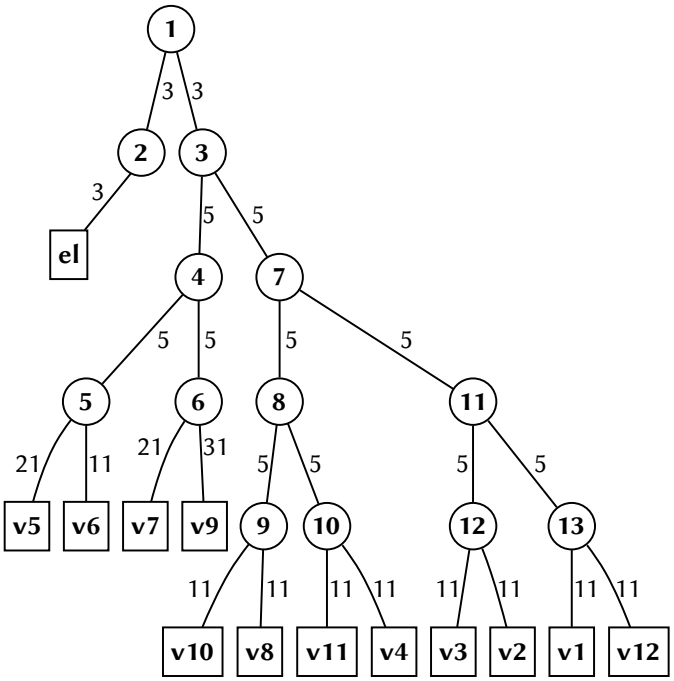

Figure S1 Largest SPF basis used for the ML-MCTDH dynamics of IC1 ethylene on the LVC potentials. The numbers on the last layer correspond to the number of primitive harmonic oscillator DVR functions used.

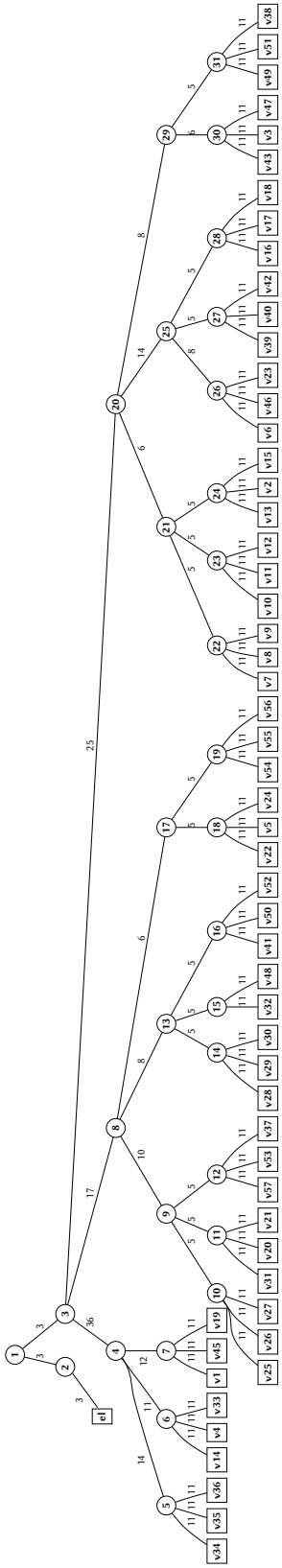

Figure S2 Largest SPF basis used for the ML-MCTDH dynamics of IC2 DMABN on the LVC potentials. The numbers on the last layer correspond to the number of primitive harmonic oscillator DVR functions used.

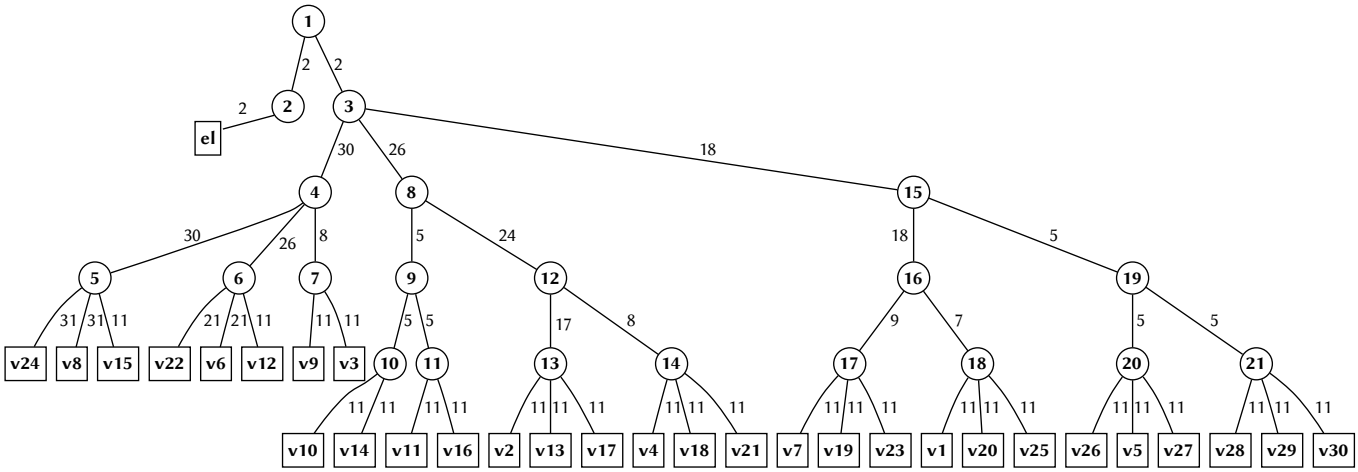

Figure S3 Largest SPF basis used for the ML-MCTDH dynamics of IC3 fulvene on the LVC potentials. The numbers on the last layer correspond to the number of primitive harmonic oscillator DVR functions used.

S5 Geometries of the Molecules at the Conical Intersections

Table S10 Minimum energy conical intersection between states S_1 and S_2, in Cartesian coordinates (in Å), of ethene taken from the dynamics database potentials.

C	-0.008033	-0.680656	0.003929
C	0.002923	0.674370	0.013231
H	0.709421	-1.112851	-0.730160
H	-0.694334	-1.236853	0.658034
H	0.692786	1.218795	0.627922
H	-0.646988	1.205814	-0.760273

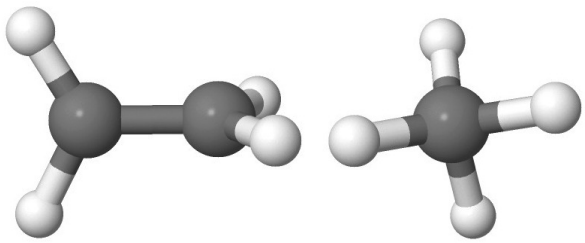

Figure S4 Minimum energy conical intersection between states S_1 and S_2, of ethene from the dynamics database potentials

Table S11 Minimum energy conical intersection between states S_0 and S_1, in Cartesian coordinates (in Å), of ethene taken from the dynamics database potentials.

C	0.100643	-1.375462	-0.233367
C	-0.063276	1.452296	0.174959
H	0.646177	-2.425109	1.050178
H	-1.018896	-1.346184	0.619764
H	1.030552	1.454470	-0.702185
H	-1.103063	1.401279	-0.271771

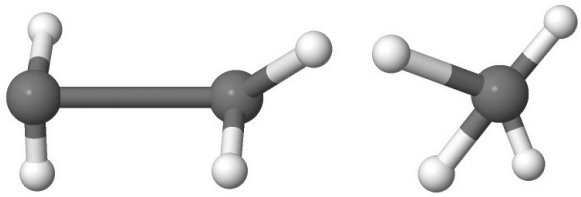

Figure S5 Mimimum energy conical intersection between states S_0 and S_1, of ethene from the dynamics database potentials.

Table S12 Comparison of the normal mode coordinates of the minimum energy conical intersection between states S_1 and S_2 for ethene from the LVC model and the DD-vMCG potentials.

	Normal Mode Coordinate	
Mode	LVC	DD-vMCG
v_1	0.00000	0.33226
v_2	0.00000	-0.21166
v_3	0.00000	-0.64567
v_4	0.00004	-0.41130
v_5	-3.54784	-0.55934
v_6	-0.00000	0.35548
v_7	-3.06464	1.19622
v_8	0.00000	-11.01107
v_9	-0.00000	0.05233
v_{10}	-0.55158	-4.29818
v_{11}	-0.00002	-0.38107
v_{12}	-0.00000	0.00703

Table S13 Minimum energy conical intersection, in Cartesian coordinates (in Å), between states S_1 and S_2 of DMABN, taken from the dynamics database potentials.

C	3.024509	-1.240828	-0.053202
N	2.311406	-0.001309	0.109433
C	0.924761	0.001395	0.050468
C	0.167591	-1.213849	0.024264
C	-1.178039	-1.214803	0.003590
C	-1.936117	0.002263	-0.000258
C	-1.176807	1.218886	0.006504
C	0.169123	1.218514	0.029222
H	0.685117	2.175891	0.031455
H	-1.711497	2.166576	-0.015362
C	-3.336139	0.000554	-0.017013
N	-4.516214	-0.004586	-0.029601
H	-1.712016	-2.163056	-0.010281
H	0.683575	-2.169372	0.016825
C	3.026846	1.236121	-0.059797
H	2.731126	1.992572	0.692231
H	4.099093	1.041142	0.061865
H	2.868018	1.692105	-1.063399
H	2.716856	-1.995810	0.697967
H	2.881685	-1.699717	-1.060008
H	4.098102	-1.051986	0.082546

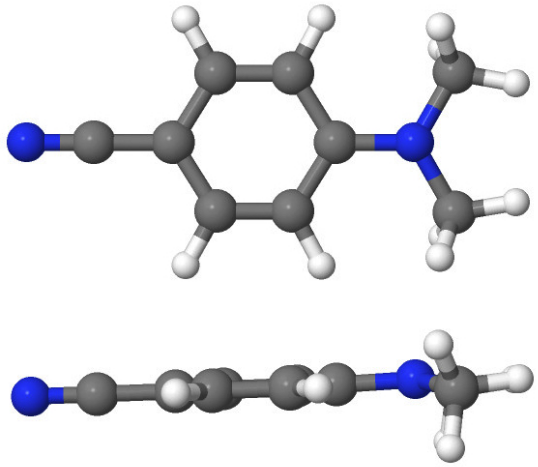

Figure S6 Mimimum energy conical intersection between states S_2 and S_3 of DMABN, from the dynamics database potentials

Table S14 Comparison of the normal mode coordinates of the minimum energy conical intersection of the S_2 and S_3 states of DMABN taken from the LVC model and DD-vMCG dynamics data

	Normal Mode Coordinate			Normal Mode Coordinate	
Mode	LVC	DD-vMCG	Mode	LVC	DD-vMCG
q_1	0.05343	0.25551	q_{30}	0.14690	0.13330
q_2	0.19418	0.06143	q_{31}	0.70029	0.57175
q_3	0.42462	0.19868	q_{32}	-0.21560	-0.00944
q_4	0.04447	-0.00580	q_{33}	0.00071	0.00014
q_5	0.15069	0.04466	q_{34}	-0.00261	0.00151
q_6	0.02069	-0.00691	q_{35}	-0.00132	0.00880
q_7	-0.03828	-0.00537	q_{36}	0.20816	0.24245
q_8	-0.16589	-0.03621	q_{37}	0.00310	-0.01522
q_9	0.38585	0.15609	q_{38}	0.00120	-0.01328
q_{10}	0.00718	-0.02757	q_{39}	-0.01796	-0.02500
q_{11}	-0.00414	-0.02002	q_{40}	0.05473	0.04427
q_{12}	0.28074	0.04826	q_{41}	-0.00553	-0.00688
q_{13}	0.13323	0.02080	q_{42}	-0.00181	0.00763
q_{14}	0.00097	0.01345	q_{43}	0.14007	0.14505
q_{15}	0.04425	0.01512	q_{44}	-0.49346	-0.37440
q_{16}	-0.00265	0.00679	q_{45}	-0.00079	-0.00385
q_{17}	0.14531	0.06100	q_{46}	0.98669	0.99337
q_{18}	0.08844	0.05069	q_{47}	0.47848	0.47945
q_{19}	0.61324	0.09655	q_{48}	-0.00317	-0.01493
q_{20}	-0.00294	-0.00419	q_{49}	-0.10873	-0.08274
q_{21}	-0.03711	-0.03920	q_{50}	-0.00246	0.00093
q_{22}	0.29439	0.08675	q_{51}	-0.00561	-0.00882
q_{23}	-0.40303	-0.12405	q_{52}	0.00093	0.00165
q_{24}	0.00020	0.03656	q_{53}	-0.03516	-0.02270
q_{25}	0.12662	0.03467	q_{54}	0.03130	0.03041
q_{26}	0.00123	-0.00226	q_{55}	-0.01166	-0.01378
q_{27}	0.10862	0.11113	q_{56}	-0.00010	0.01099
q_{28}	-0.02740	-0.04254	q_{57}	0.02153	-0.02703
q_{29}	-0.01307	-0.01122			

Table S15 Minimum energy conical intersection in Cartesian coordinates (in Å) of the S_0 and S_1 states of fulvene taken from the dynamics database potentials

C	-0.000053	1.102171	-0.065221
C	0.000078	0.646263	-1.522348
C	0.000368	-0.645872	-1.522935
C	0.001107	-1.103406	-0.066112
C	-0.000437	-0.000737	0.729923
C	-0.001055	0.001148	2.267389
H	0.001306	-0.917628	2.810638
H	0.001240	0.923555	2.803640
H	0.001466	-2.113285	0.288844
H	-0.007532	-1.297010	-2.373363
H	-0.003840	1.299140	-2.371137
H	0.007253	2.110393	0.294352

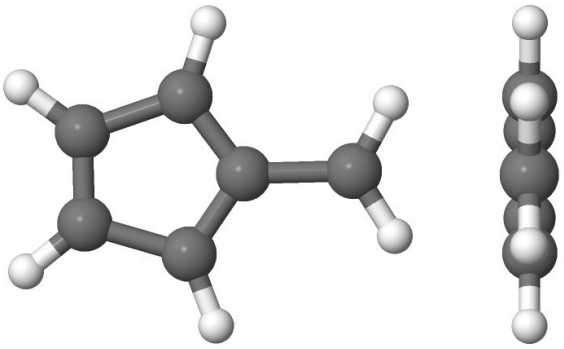

Figure S7 Minimum energy conical intersection of fulvene, taken from the dynamics database

Table S16 Comparison of the normal mode coordinates of the minimum energy conical intersection of the S_0 and S_1 states of fulvene, taken from the LVC and DD-vMCG dynamics data

	Normal Mode Coordinate	
Mode	LVC	DD-vMCG
q_1	0.00000	-0.01210
q_2	0.00000	0.03246
q_3	0.00000	-0.01107
q_4	0.00000	-0.00913
q_5	0.00000	-0.01936
q_6	2.55690	2.76994
q_7	0.00000	-0.01989
q_8	0.00000	-0.01112
q_9	0.00000	-0.00259
q_{10}	0.00000	0.03444
q_{11}	0.00000	0.00343
q_{12}	0.00000	0.03285
q_{13}	-1.96350	-1.59851
q_{14}	0.00000	0.00435
q_{15}	-2.21243	-1.61462
q_{16}	0.00000	-0.00414
q_{17}	1.76322	2.56636
q_{18}	0.00000	0.01640
q_{19}	0.00000	-0.00372
q_{20}	-0.95906	-1.02351
q_{21}	0.49381	0.88174
q_{22}	2.58957	3.03345
q_{23}	0.00000	0.00279
q_{24}	-3.08090	-3.29134
q_{25}	0.19601	0.23302
q_{26}	0.00000	-0.00414
q_{27}	0.00000	0.00017
q_{28}	-0.04144	0.02233
q_{29}	0.00000	-0.00239
q_{30}	-0.05960	0.00731

S6 Convergence of vMCG and partitioned vMCG (G-MCTDH).

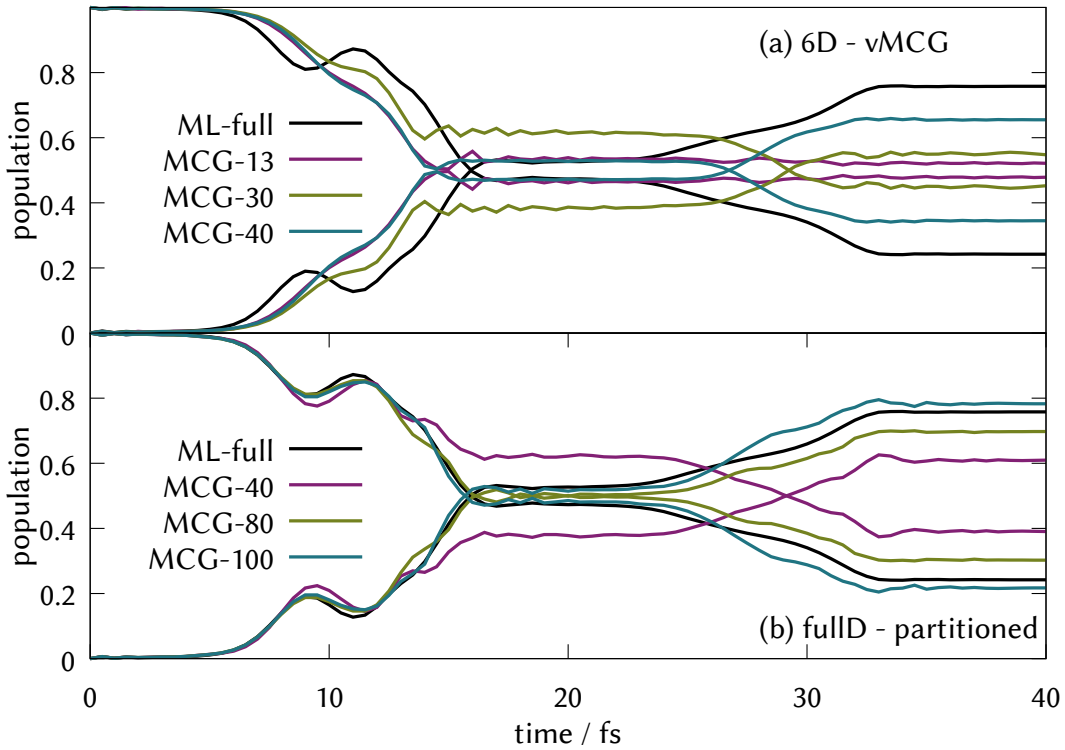

Figure S8 Convergence of vMCG and partitioned vMCG for the diabatic state populations of the fulvene LVC Hamiltonian. (a) vMCG calculations with different numbers of full dimensional basis functions for a 6D model. Approaching convergence on the exact MCTDH result (ML-full) with 40 GWPs. (b) Partitioned vMCG (G-MCTDH) calculations with different numbers of basis functions. The modes are partitioned as in Table 1 of the paper and the number of GWPs changed for the first partition, keeping 40 GWPs for the second partition in all calcualtions. Convergence against the full ML-MCTDH result (ML-full) is seen for a basis of (100,40), i.e. 4000 configurations.

S7 The validity of the adiabatic populations from vMCG

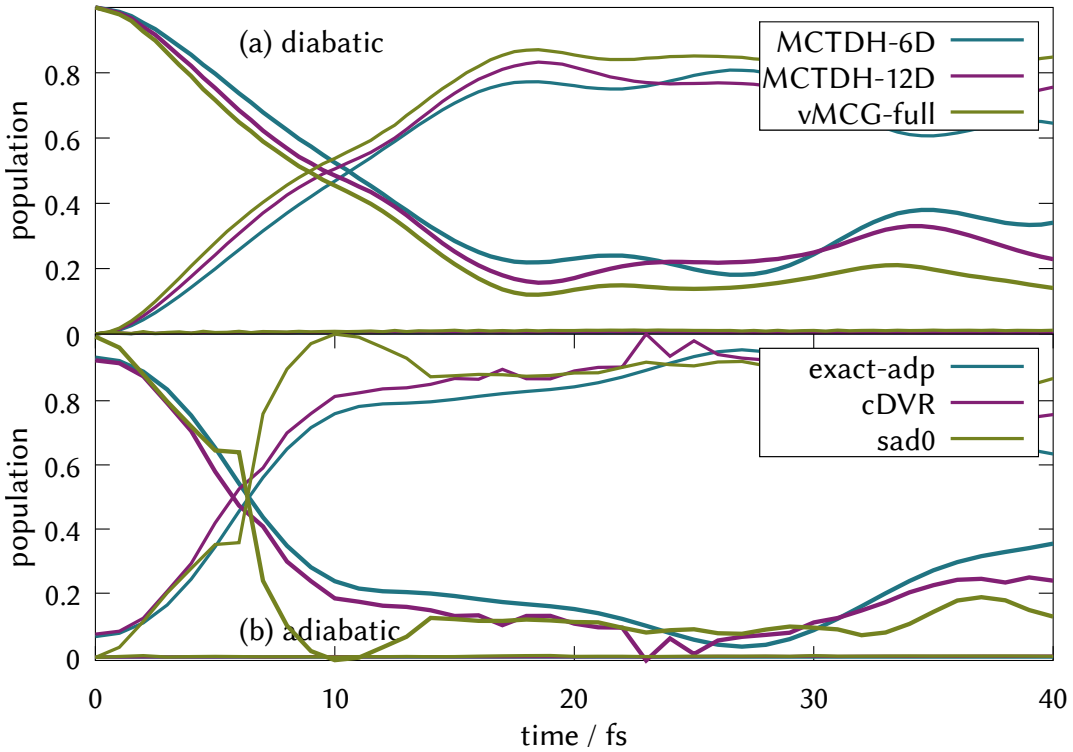

Figure S9 The (a) diabatic and (b) adiabatic populations for reduced dimensionality models of IC2 (DMABN) using the LVC Hamiltonian. In (a), the difference in diabatic populations for 6D and 12D models are compared to the full dimensional calculation. In (b), the exact adiabatic populations for the 6D model from an MCTDH calculation are shown (exact-adp), along with a correlation DVR approximation used on the same simulation (cDVR) which is seen to perform well. The adiabatic populations from a 6D vMCG calculation using the saddle-point approximation (sad0) are seen to deviate when passing through the intersection, but to otherwise provide a good approximation for the populations.

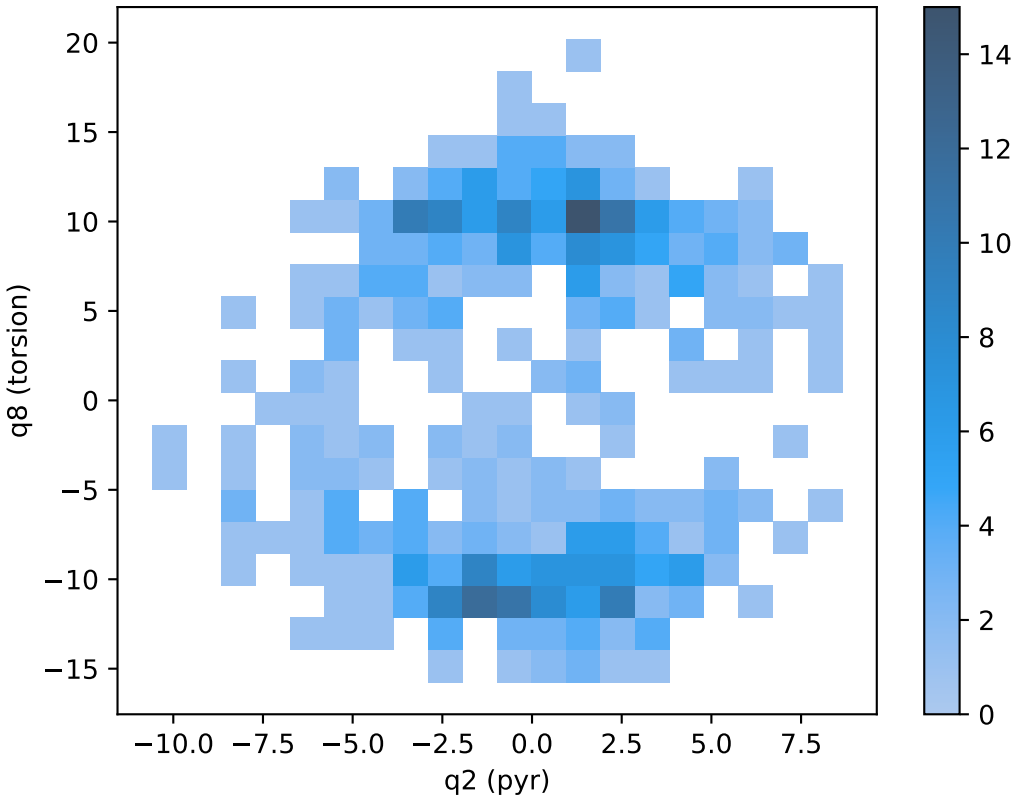

Figure S10 Heatmap corresponding to the hopping geometries extracted from the Tully surface hopping trajectories in the IC1 model (ethene) and projected onto the q_2 pyramidalisation and q_8 torsional modes. The values have been binned (n=20) and the z axis corresponds to the number of values in the interval. The most visited geometries correspond to values around q_8=9-12 and q_2=0-3 .

Table S17 Representative (average) "hopping" geometry, in Cartesian coordinates (in Å), of ethene taken from the geometries where hops take place in the DD-TSH calculations. Used to define the cut through the potentials in Fig. 8.

C	-0.002719	-0.826984	0.017367
C	-0.054046	0.805890	-0.070521
H	1.111156	-1.298427	0.646442
H	-0.686581	-1.195414	-0.614285
H	0.700451	1.083783	-0.329751
H	-0.448625	1.661427	0.930976

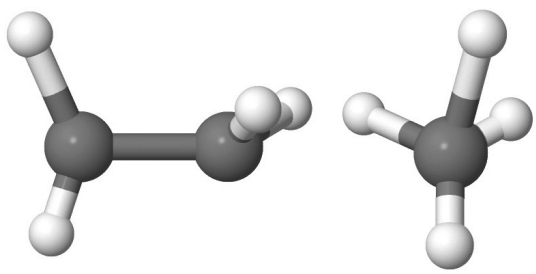

Figure S11 Representative (average) "hopping" geometry of ethene taken from the geometries where hops take place in the DD-TSH calculations.

S8 Loss of Wavepacket Symmetry in DD-vMCG Simulation of IC1

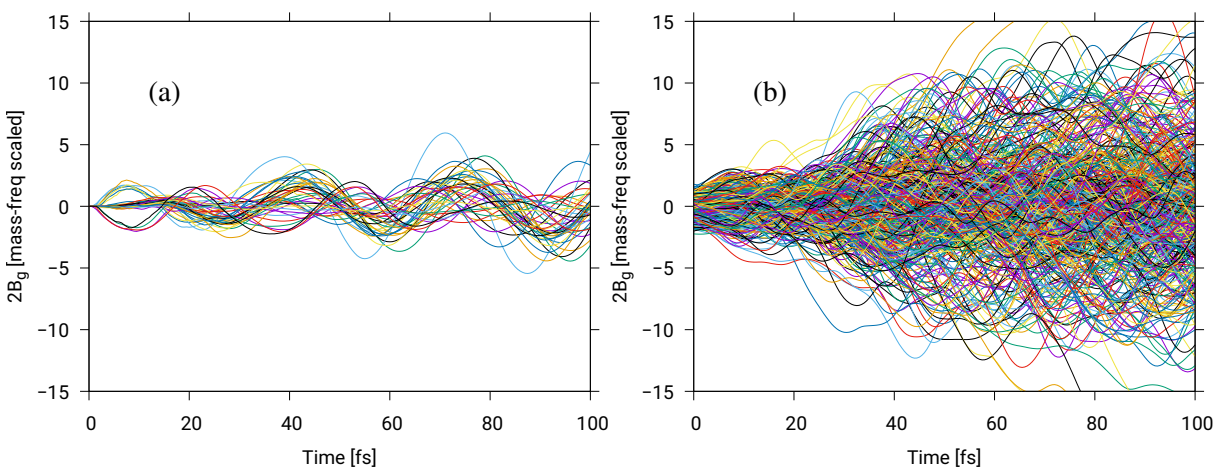

Figure S12 The values of the pyramidalisation (q_2) coordinate taken from simulations of the IC1 model. (a) The centre of the GWP basis functions from DD-vMCG and (b) Trajectories from DD-TSH. The symmetry is lost in DD-vMCG after an oscillation but the wavefunction remains compact (see Fig. 7 for the full density of the wavepacket on top of the trajectories).

S9 Datasets of Calculations Available

The data from the calculations are available at DOI: 10.5522/04/23807676. They are in the form of zipped tar files containing all the input and output files for the calculations described in the paper.

ethene_lvc.tar.gz	LVC model of IC1 (ethene). MCTDH, vMCG and TSH calculations.
dmabn_lvc.tar.gz	LVC model of IC2 (DMABN). MCTDH, vMCG and TSH calculations.
fulvene_lvc.tar.gz	LVC model of IC3 (fulvene). MCTDH, vMCG and TSH calculations.
ethene_direct.tar.gz	Direct dynamics of IC1 (ethene). DD-vMCG and DD-TSH calculations. Includes the potential energy database (ethene_DB)
dmabn_direct.tar.gz	Direct dynamics of IC2 (DMABN). DD-vMCG and DD-TSH calculations. Includes the potential energy database (dmabn_DB)
fulvene_direct.tar.gz	Direct dynamics of IC3 (fulvene). DD-vMCG and DD-TSH calculations. Includes the potential energy database (fulvene_db)